

See discussions, stats, and author profiles for this publication at: <https://www.researchgate.net/publication/231637724>

# Lifetimes and Modes of Decay of Sulfur-Centered Radical Zwitterions Containing Carboxylate and Phenyl Groups

ARTICLE *in* THE JOURNAL OF PHYSICAL CHEMISTRY A · JUNE 2004

Impact Factor: 2.69 · DOI: 10.1021/jp036962k

CITATIONS

21

READS

30

6 AUTHORS, INCLUDING:



**Piotr Filipiak**

Adam Mickiewicz University

18 PUBLICATIONS 168 CITATIONS

SEE PROFILE



**Lily Hug**

University of Greenwich

114 PUBLICATIONS 2,665 CITATIONS

SEE PROFILE



**Krzysztof Bobrowski**

Instytut Chemii i Techniki Jądrowej

129 PUBLICATIONS 2,051 CITATIONS

SEE PROFILE

# Lifetimes and Modes of Decay of Sulfur-Centered Radical Zwitterions Containing Carboxylate and Phenyl Groups

Piotr Filipiak,<sup>†,‡</sup> Gordon L. Hug,<sup>‡</sup> Ian Carmichael,<sup>‡</sup> Anna Korzeniowska-Sobczuk,<sup>§</sup> Krzysztof Bobrowski,<sup>§</sup> and Bronisław Marciniak<sup>\*,†</sup>

Faculty of Chemistry, Adam Mickiewicz University, 60-780 Poznań, Poland, Radiation Laboratory, University of Notre Dame, Notre Dame, Indiana 46556, and Institute of Nuclear Chemistry and Technology, Dorodna 16, 03-195 Warsaw, Poland

Received: October 3, 2003; In Final Form: February 20, 2004

The fates of sulfur-centered radical zwitterions were determined following triplet-sensitized electron transfer from thioether-containing aromatic carboxylic acids. 4-Carboxybenzophenone was used as the triplet sensitizer and four carboxylic acids, (phenylthio)acetic acid (**1**), *S*-benzylthioglycolic acid (**2**), 4-(methylthio)phenylacetic acid (**3**), and 4-(methylthio)benzoic acid (**4**), were the electron-donating quenchers. Following laser-induced electron transfer, the time development of the ensuing free-radical reactions was monitored by optical spectroscopy. The reference spectra of the photoinduced transients were selectively generated by a complementary pulse radiolytic method in order to determine extinction coefficients and spectral shapes. By use of these reference spectra, the observed transient spectra from laser flash photolysis were resolved into their components. From this information, concentration profiles and initial quantum yields of the radicals were determined along with triplet quenching rate constants. The chemistry of the free radicals was discussed with the aid of computations from density functional theory (DFT). DFT also was used to supplement the spectral assignments as well as for computation of the thermochemistry of the free radicals. The sulfur-centered radical zwitterions from **1** and **2** decayed rapidly. Those from **1** decayed into  $\cdot\text{CH}_2\text{-S-C}_6\text{H}_5$  and  $\text{CO}_2$ . A majority of those from **2** also decayed via decarboxylation but, in addition, through fragmentation. The  $\text{CH}_3\text{-S}^+\text{-C}_6\text{H}_4\text{-CH}_2\text{-CO}_2^-$  radicals from **3** could be observed directly for microseconds and decayed with roughly equal probability through decarboxylation and deprotonation. The  $\text{CH}_3\text{-S}^+\text{-C}_6\text{H}_4\text{-CO}_2^-$  radicals from **4** were also observed directly but failed to decarboxylate because of the high energy of activation needed to form the substituted phenyl radical.

## Introduction

Free radicals and radical ions, having their unpaired spins mainly on sulfur atoms, play unique roles in diverse areas of chemistry. They are important intermediates for specialized organic synthesis.<sup>1–3</sup> In oxidative stress,<sup>4</sup> they are implicated in the early stages of oxidative attack associated with aging<sup>5</sup> and with pathologies such as Alzheimer's disease.<sup>6</sup> Sulfur-centered radicals are also involved in environmental issues.<sup>7–9</sup> Recently sulfur-centered radicals derived from co-initiators have proven to be effective in photopolymerizations.<sup>10</sup>

Sulfur radical cations from thioethers are quite reactive, which raises the question of how oxidative damage can be stabilized in oxidative stress.<sup>6</sup> On the other hand, it is the reactivity of the sulfur radical cations that is important in photopolymerization.<sup>10</sup> In this regard, it is not the reactivity of these radical cations, themselves, that is important since they appear to be only mild oxidants.<sup>11</sup> What is significant for effective free-radical polymerization is the tendency for sulfur radical cations to deprotonate,<sup>12</sup> forming carbon-centered radical sites adjacent to the sulfur atoms. For initiating free-radical polymerization, another mode of reactivity that is very important is the decarboxylation of sulfur-containing carboxylic acids.<sup>10</sup>

One convenient detection method for monitoring sulfur radical cations is transient absorption spectroscopy. Unfortunately, sulfur radical cations from purely alkyl thioethers have only very weak absorptions in the near UV (even though they form strongly absorbing dimers<sup>11</sup> with two-centered, three-electron bonds with unreacted thioether molecules).<sup>13</sup> On the other hand, monomeric sulfur radical cations from thioethers, containing aromatic moieties, do absorb in the visible.<sup>14,15</sup> This feature of aromatic thioethers makes them ideal precursors of sulfur radical cations that can be used for probing mechanisms of electron-transfer quenching of excited states (forming sulfur radical cations) as well as for monitoring the fate of the sulfur radicals.

In the present work we use this approach. Of particular interest is the recent use of sulfur radical cations to produce carbon-centered radicals that can initiate free radical polymerizations. A water-soluble benzophenone, 4-carboxybenzophenone (CB), is used as the photosensitizer, and four different aromatic thioethers are used as quenchers. Optical detection is used to follow the fate of transients produced in quenching events initiated by time-resolved laser flash photolysis. The transient absorptions are characterized quantitatively by generating radicals from the aromatic thioethers by use of optically detected pulse radiolysis. A similar procedure has been used for sulfur-containing aliphatic carboxylic acids.<sup>16</sup>

The mechanism describing the primary photochemical processes involved in the electron-transfer quenching of the triplet

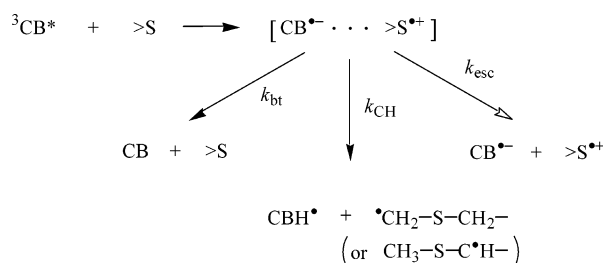
\* To whom correspondence should be addressed: e-mail marcinia@amu.edu.pl.

<sup>†</sup> Adam Mickiewicz University.

<sup>‡</sup> Notre Dame Radiation Laboratory.

<sup>§</sup> Institute of Nuclear Chemistry and Technology.

## SCHEME 1



state of CB by sulfur-containing organic compounds has been studied.<sup>17</sup> The general reaction mechanism is shown in Scheme 1. After an initial formation of a radical ion pair, there are three main channels of its decay: (i) back electron transfer to form the reactants in their ground states, (ii) proton transfer within the radical ion pair to form the ketyl radical (CBH<sup>•</sup>) and an  $\alpha$ -alkyl thioalkyl radical, and (iii) escape of the ion radicals to form CB<sup>•−</sup> and the sulfur-centered radical cation (S<sup>•+</sup>, which will stand for S-centered radical zwitterions in the present work; see below). Further secondary reactions depend on the structure of the sulfur-containing organic compounds used.<sup>17</sup> In the present work, mechanisms of the free-radical reactions after the triplet quenching events are elucidated.

## Experimental Section

**Materials.** 4-Carboxybenzophenone was from Aldrich. (Phenylthio)acetic acid (1), C<sub>6</sub>H<sub>5</sub>-S-CH<sub>2</sub>-COOH; *S*-benzylthioglycolic acid (2), C<sub>6</sub>H<sub>5</sub>-CH<sub>2</sub>-S-CH<sub>2</sub>-COOH; 4-(methylthio)phenylacetic acid (3), *p*-CH<sub>3</sub>-S-C<sub>6</sub>H<sub>4</sub>-CH<sub>2</sub>-COOH; and 4-(methylthio)benzoic acid (4), *p*-CH<sub>3</sub>-S-C<sub>6</sub>H<sub>4</sub>-COOH, were purchased from both Aldrich and Lancaster. The deionized water was purified in a reverse osmosis/deionization system from Serv-A-Pure Co. There was a UV-irradiation unit in the circulating section of this water-purification system. The water had a resistance >18 M $\Omega$ /cm and a total organic carbon (TOC) content of <10 ppb.

**Laser Flash Photolysis.** The nanosecond laser flash photolysis and its data acquisition system have been previously described in detail.<sup>18</sup> The nitrogen laser provided 8 ns, 6 mJ pulses at 337 nm. The transients were monitored with a pulsed 1 kW xenon lamp, having the monitoring beam perpendicular to the laser beam. All experiments were carried out with a gravity-driven flow system and a rectangular quartz optical cell (0.5  $\times$  1 cm). The monitoring light path length, *l*, was 0.5 cm. A solution of CB (2 mM) at neutral pH was used as the actinometer.

**Pulse Radiolysis.** A Titan Beta model TBS 8/16-1S linear accelerator at the Notre Dame Radiation Laboratory provided 2–3 ns pulses of 8 MeV electrons<sup>19</sup> and the 10-MeV LAE 10 electron accelerator at the Institute of Nuclear Chemistry and Technology in Warsaw<sup>20</sup> provided 8 ns pulses. Transients were also monitored by a pulsed 1 kW xenon lamp. The radiolysis cell was quartz with the monitoring light path length of 1 cm. A peristaltic pump drove the flow in the sample delivery system. The data acquisition system allows for kinetic traces to be displayed on multiple time scales and has been described previously.<sup>19,20</sup> Absorbed doses per pulse were on the order of 6 Gy (1 Gy = 1 J kg<sup>−1</sup>). Dosimetry was based on N<sub>2</sub>O-saturated solutions containing 10<sup>−2</sup> M KSCN, taking a radiation chemical yield of *G* = 6.13 radicals produced per 100 eV of absorbed energy (0.635  $\mu\text{M J}^{-1}$ ) and a molar extinction coefficient of 7580 M<sup>−1</sup> cm<sup>−1</sup> at 472 nm for the (SCN)<sub>2</sub><sup>•−</sup> radical.<sup>21</sup> An absorbed dose of 6 Gy produces [(SCN)<sub>2</sub><sup>•−</sup>] = 3.5  $\mu\text{M}$  in N<sub>2</sub>O-saturated aqueous solutions based on *G* = 6.13.

**Computational Details.** Density functional theory (DFT) calculations were performed with the Gaussian98 electronic structure software package<sup>22</sup> employing the popular B3LYP functional.<sup>23</sup> This hybrid functional comprises both local<sup>24</sup> and nonlocal<sup>25</sup> (gradient-corrected) exchange and correlation<sup>26,27</sup> contributions mixed with a piece of exact (Hartree–Fock) exchange. The mixing parameters were derived from fits to known thermochemistry of a well-characterized set of small molecules. For open-shell systems (the transient radicals and radical cations) spin-unrestricted DFT (UB3LYP) was employed. For structural studies the (heavy-atom) polarized split-valence 6-31G\* basis set<sup>28</sup> was used. DFT geometries are often converged with modest basis sets. Vertical excited states were located by use of time-dependent density functional response theory within the random phase approximation.<sup>29</sup> TD-UB3LYP often performs well for valence states but can have difficulties with Rydberg transitions due to the incorrect asymptotic functional behavior. To locate the absorption maxima and estimate the transition strength, diffuse functions were added to the heavy atom basis, 6-31+G\*. The characteristics of the charge distributions in the neutral and ionized species were mapped with a natural population analysis from the NBO component<sup>30</sup> of Gaussian98, and dipole moments were obtained as expectation values. Solvent effects were modeled by self-consistent reaction field theory with a polarized cavity model<sup>31</sup> with COSMO boundary conditions.<sup>32</sup>

## Results and Discussion

**Spectral Resolutions.** Aqueous solutions of CB and the four quenchers were excited at 337 nm under flash photolysis. For each solution, a set of kinetic traces was collected for a sequence of monitoring wavelengths between 360 and 800 nm at 10-nm intervals. For each individual kinetic trace acquired, the data-acquisition system automatically generates 10 derivative, kinetic traces on 10 distinct time scales.<sup>18</sup> This redundancy of time scales makes it relatively easy to assemble transient spectra at convenient time delays following the laser pulse.

After the transient spectra were assembled, each of these spectra was decomposed into component spectra associated with the various transient species present.<sup>33</sup> These spectral resolutions were made by fitting the reference spectra from, for example, pulse radiolysis (see below) to the observed transient spectra via a multiple linear regression of the form<sup>33</sup>

$$\Delta A(\lambda_i) = \sum_j \epsilon_j(\lambda_i) a_j \quad (1)$$

where  $\epsilon_j$  is the extinction coefficient of the *j*th species and regression parameters, *a<sub>j</sub>*, are equal to the concentration of the *j*th species times the optical path length of the monitoring light. The sum in eq 1 is over all species present. For any particular time delay of an experiment, the regression analysis included equations such as eq 1 for each  $\lambda_i$  under consideration. A sample spectral resolution is shown in Figure 1.

By use of this spectral-resolution technique, concentrations of the transients can be determined at any desired time delay following the laser pulse. The resulting concentration profiles for all four types of <sup>3</sup>CB\* quenching experiments are shown in Figures 2–4. In these figures, extrapolations are made back to time zero in order to make estimates of the initial quantum yields. Relative actinometry is used with separate cells of CB at a concentration such that the optical densities at 337 nm are matched in the CB actinometry cell and the quenching solution cell.<sup>34</sup> For the quenchers C<sub>6</sub>H<sub>5</sub>-S-CH<sub>2</sub>-CO<sub>2</sub><sup>−</sup> and C<sub>6</sub>H<sub>5</sub>-CH<sub>2</sub>-S-CH<sub>2</sub>-CO<sub>2</sub><sup>−</sup>, there was no problem with their absorbing the laser

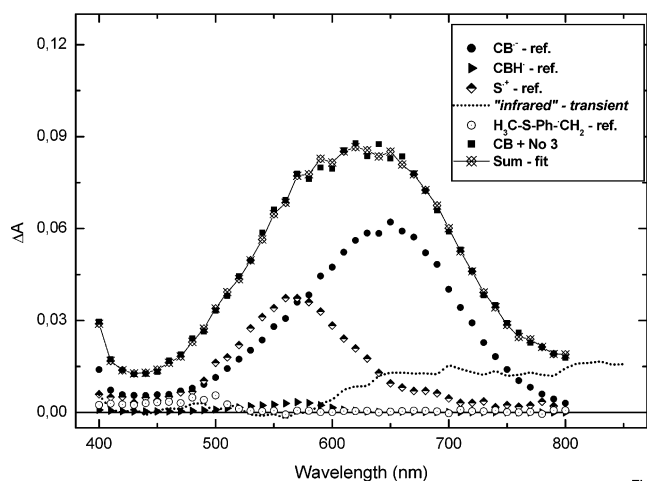


**Figure 1.** Spectral resolution of transient spectra following triplet quenching of CB by  $\text{CH}_3\text{-S-C}_6\text{H}_5\text{-CH}_2\text{-CO}_2^-$  (**3**) (5 mM) + CB (4 mM). Data were recorded 4.5  $\mu\text{s}$  after laser pulse for Ar-saturated aqueous solution, pH = 6.88; actinometry,  $[T] = 24.6 \mu\text{M}$ .

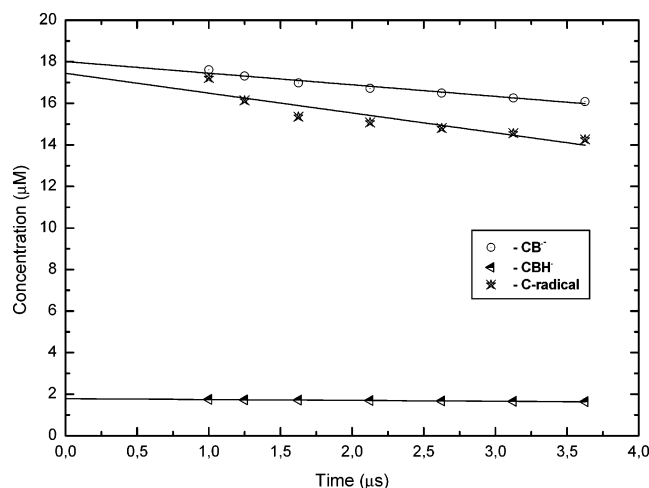


**Figure 2.** Concentration profiles of product formation following triplet quenching of CB by  $\text{C}_6\text{H}_5\text{-S-CH}_2\text{-CO}_2^-$  (**1**) (20 mM) + CB (2 mM) in Ar-saturated aqueous solution, pH = 7.5; actinometry,  $[T] = 18.6 \mu\text{M}$ .

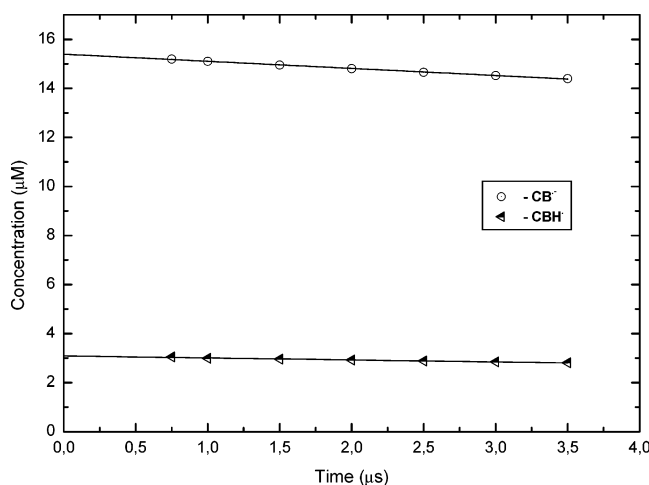


**Figure 3.** Concentration profiles of product formation following triplet quenching of CB by  $\text{C}_6\text{H}_5\text{-CH}_2\text{-S-CH}_2\text{-CO}_2^-$  (**2**) (20 mM) + CB (2 mM) in Ar-saturated aqueous solution, pH = 7.5, actinometry,  $[T] = 18.6 \mu\text{M}$ .

light; only CB absorbed the 337 nm laser beam in their presence. However,  $p\text{-CH}_3\text{-S-C}_6\text{H}_4\text{-CH}_2\text{-CO}_2^-$  and  $p\text{-CH}_3\text{-S-C}_6\text{H}_4\text{-CO}_2^-$  both absorb significant fractions of the laser light when either

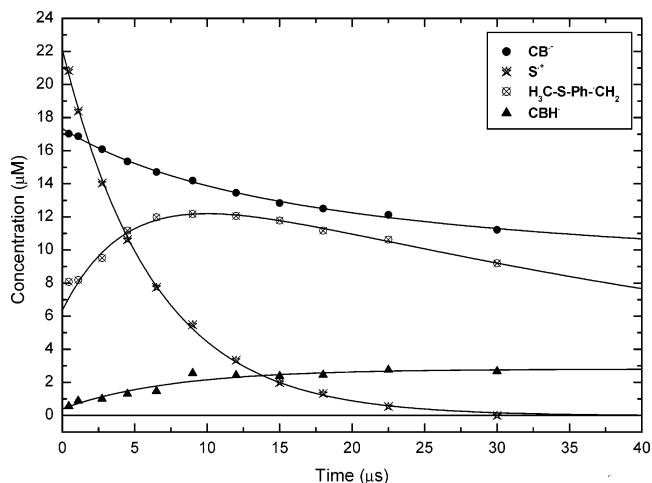


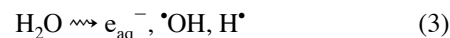
**Figure 4.** Concentration profiles of product formation following triplet quenching of CB by  $\text{CH}_3\text{-S-C}_6\text{H}_4\text{-CH}_2\text{-CO}_2^-$  (**3**) (5 mM) + CB (4 mM) in Ar-saturated aqueous solution, pH = 6.88, actinometry,  $[T] = 24.6 \mu\text{M}$ .

of these two anions is present at the concentrations used in the quenching experiments. To get estimates of the light absorbed by CB in the presence of these latter two quenchers, an inner-filter effect<sup>35</sup> correction was made:

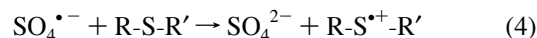
$$f_a = \left( \frac{\epsilon_{\text{CB}} c_{\text{CB}}}{\epsilon_{\text{CB}} c_{\text{CB}} + \epsilon_{\text{Q}} c_{\text{Q}}} \right) \left( \frac{1 - \exp\{-2.3(\epsilon_{\text{CB}} c_{\text{CB}} + \epsilon_{\text{Q}} c_{\text{Q}})l\}}{1 - \exp\{-2.3\epsilon_{\text{CB}} c_{\text{CB}} l\}} \right) \quad (2)$$

In eq 2,  $\epsilon_{\text{CB}}$  and  $\epsilon_{\text{Q}}$  are the respective extinction coefficients (at 337 nm) of the ground states of CB and Q;  $c_{\text{CB}}$  and  $c_{\text{Q}}$  are their ground-state concentrations in the quenching experiments;  $l$  is the optical path length of the laser through the cell; and  $f_a$  is the fraction of light absorbed by the ground state of CB in the presence of the quenchers. Initial quantum yields, computed from the concentration profiles extrapolated to zero time delay and corrected for inner-filter effects, are reported in Table 1. For reference to the interpretations of these quantum yields (see below), the previously<sup>10</sup> measured quantum yields of decarboxylation ( $\text{CO}_2$  formation) are also listed in Table 1.

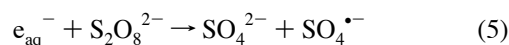
**Reference Spectra from Pulse Radiolysis.** In an attempt to characterize sulfur-centered radical zwitterions of the aromatic thioether carboxylates, we employed a pulse radiolysis technique that was used previously<sup>15,36</sup> to study radical cations from aromatic thioethers. Pulse radiolysis of water yields primary species



with relative yields of approximately 2.65:2.65:0.6, respectively. To form radical cations from thioethers, the  $\text{SO}_4^{\bullet-}$  radical was used as an one-electron oxidizing agent



where the radical anions,  $\text{SO}_4^{\bullet-}$ , were formed by scavenging hydrated electrons,  $e_{\text{aq}}^-$ , by 2 mM  $\text{S}_2\text{O}_8^{2-}$



with  $k_5 = 1.2 \times 10^{10} \text{ M}^{-1} \text{ s}^{-1}$ .<sup>37</sup> The hydroxyl radicals were scavenged by the reactions with *tert*-butyl alcohol, which was present in large concentrations, 0.1 M, forming a relatively unreactive C-centered radical,  $\cdot\text{CH}_2\text{C}(\text{CH}_3)_2\text{OH}$ :



**TABLE 1: Rate Constants for Quenching of the CB Triplet and Quantum Yields<sup>a</sup> Following CB Triplet Quenching in Water, pH 7**

quencher	$k_q \times 10^{-9} \text{ (M}^{-1} \text{ s}^{-1}\text{)}$	$\Phi_{\text{CO}_2^b}$	$\Phi_{\text{CB}^{\bullet-} c}$	$\Phi_{\text{CBH}^{\bullet} c}$	$\Phi_{\text{S}^{\bullet+} c}$	$\Phi_{\text{C}^{\bullet d}}$
1, phenyl(thioacetic) acid	1.9	0.92	$0.97 \pm 5\%$	$0.10 \pm 19\%$	e	$0.93 \pm 11\%^c$
2, S-benzylthioglycolic acid	1.5	0.57	$0.83 \pm 6\%$	$0.17 \pm 6\%$	e	f
3, 4-(methylthio)phenylacetic acid	1.9	0.40 <sup>g</sup>	$0.71 \pm 4\%^h$	$0.017 \pm 10\%^h$	$0.90 \pm 7\%^h$	$\approx 0.5^i$
4, 4-(methylthio)benzoic acid	1.9	<0.05	nd <sup>j</sup>	nd <sup>j</sup>	nd <sup>j</sup>	nd <sup>j</sup>

<sup>a</sup>  $a_j = c_j \times l$  ( $l = 0.5 \text{ cm}$ )  $- a_j$  - data from spectra resolution  $\rightarrow c_j = a_j/l$ . From (T-T) absorption spectra, the actinometry is  $[T] = \Delta A_{535}/(\epsilon_{535} \times l)$  ( $\epsilon_{535} = 6250 \text{ M}^{-1} \text{ cm}^{-1}$ )  $\Phi_j = c_j/[T]$  for the  $j$ th species. <sup>b</sup> Quantum yield for formation of carbon dioxide, from steady-state measurements, extrapolated to 0% CB conversion; estimated errors  $\pm 10\%$ . <sup>c</sup> Quantum yields for the formation of CB radical anion, CB ketyl radical, and S-centered radical zwitterion, from laser flash photolysis extrapolated to the end of the flash; estimated from spectral resolution. <sup>d</sup> Quantum yield for the formation of C-centered radicals (decarboxylated). <sup>e</sup>  $\text{S}^{\bullet+}$ ; its lifetime is so short that is difficult to get initial yields for  $\text{S}^{\bullet+}$ . <sup>f</sup> Could not be detected. <sup>g</sup>  $f_a = 0.724$ , from inner-filter effect (eq 2), at 313 nm. <sup>h</sup>  $f_a = 0.897$ , from inner-filter effect (eq 2), at 337 nm. <sup>i</sup> Taken at the maximum of the growth/decay concentration profile. <sup>j</sup> Not determined.



The pH was adjusted to 5.5 with  $\text{HClO}_4$  in order to keep the concentration of protons low enough so that hydrated electrons would react with  $\text{Na}_2\text{S}_2\text{O}_8$  instead of with protons. The solutions were degassed with nitrogen.

The dosimetry was again based on thiocyanate (see above). However, the radiation yield for the formation of  $\text{S}^{\bullet+}$ , the sulfur radical zwitterions, was taken to be  $G(\text{S}^{\bullet+}) = 2.15$ . The difference between this  $G$  and  $G(\text{SO}_4^{\bullet-}) = G(e_{\text{aq}}^-) = 2.65$  is that  $\text{SO}_4^{\bullet-}$  reacts with *tert*-butyl alcohol and with the appropriate acid via H-atom abstraction.<sup>14, 15</sup>

**Sulfur Radical Zwitterions.** The sulfur-centered radical zwitterions are formally neutral radicals formed from sulfur-containing carboxylate anions transferring their excess electron to electron acceptors, but DFT calculations show that these neutral radicals have large dipole moments. In the gas phase, the computed dipole moments are 5.5, 5, and 5.1 D for the neutral radicals from compounds **1**, **2**, and **4**, respectively. Single-point DFT calculations of the solvent effect on the dipole moments show that the dipole moments of **1** and **2** both increase by another 50%, after solvation, whereas even **4** increases by 20%. The free energy of solvation ( $\Delta G$ ) of the neutral radical of **1** is  $-10 \text{ kcal/mol}$ ; of **2**,  $-12 \text{ kcal/mol}$ ; and of **4**,  $-3 \text{ kcal/mol}$ . The large dipole moments and significant solvation energies support the notion that the neutral radicals are indeed zwitterionic and should have free radical chemistry reminiscent of true sulfur radical cations.

**Quenching of  $^3\text{CB}^*$  by  $\text{C}_6\text{H}_5\text{-S-CH}_2\text{-CO}_2^-$ .** The rate constant for the quenching of  $^3\text{CB}^*$  by  $\text{C}_6\text{H}_5\text{-S-CH}_2\text{-CO}_2^-$  was measured by varying the concentration of quencher and fitting the decay of the triplet-triplet absorption of  $^3\text{CB}^*$  at 535 nm to single-exponential decays. The equation describing the pseudo-first-order decay is

$$k_{\text{obs}} = \tau_0^{-1} + k_q[\text{Q}] \quad (7)$$

where  $k_{\text{obs}}$  is the reciprocal of the observed triplet lifetime coming from single-exponential fits to the 535-nm kinetic traces,  $\tau_0$  is the triplet lifetime of CB in the absence of quencher, and  $k_q$  is the second-order rate constant for the quenching of the triplet by the quencher, Q. The resulting rate constant of  $1.9 \times 10^9 \text{ M}^{-1} \text{ s}^{-1}$  (at pH 6.7) is quite large, which is suggestive of triplet-state quenching via electron transfer. This rate constant and others, measured in this work, are listed in Table 1.

For electron transfer in aqueous solution, it might be expected that radical ions or their decomposition products would be present in the transient spectra following laser pulses. The species expected (Scheme 1), in this case, would be radical anions of CB ( $\text{CB}^{\bullet-}$ ), their protonated form, the ketyl radical

( $\text{CBH}^{\bullet}$ ), C-centered radicals derived from the quencher ( $\alpha$ -alkylthioalkyl radicals), and sulfur-centered radical zwitterions of the quencher or degradation products from these sulfur-centered radical zwitterions (not shown in Scheme 1). The absorption spectra of the radical anion of CB and its ketyl radical have been previously well-characterized with extinction coefficients  $\epsilon(660 \text{ nm}) = 7660 \text{ M}^{-1} \text{ cm}^{-1}$  for  $\text{CB}^{\bullet-}$  and  $\epsilon(570) = 5200 \text{ M}^{-1} \text{ cm}^{-1}$  for  $\text{CBH}^{\bullet}$ .<sup>38,39</sup> These spectra and the spectrum of  $^3\text{CB}^*$  were extended to 800 nm for this work by use of laser flash photolysis.

The pulse radiolysis experiments to obtain reference spectra of radicals derived from the sulfur radical zwitterions of  $\text{C}_6\text{H}_5\text{-S-CH}_2\text{-CO}_2^-$  have been reported recently.<sup>15</sup> The prominent transient absorption that was left on the microsecond time scale was a species absorbing at 330 nm.<sup>15</sup> This species was assigned as the  $\cdot\text{CH}_2\text{-S-C}_6\text{H}_5$  radical. DFT computations (gas phase) show that the most intense transition of  $\cdot\text{CH}_2\text{-S-C}_6\text{H}_5$  is at 345 nm with an oscillator strength ( $f$ ) of 0.08. The next most intense transitions are at 298 nm ( $f = 0.015$ ). The behavior is consistent with monomeric,  $\alpha$ -aryl sulfur radical cations (or zwitterions in this case) being formed that rapidly decarboxylate, leading to the appearance of the  $\cdot\text{CH}_2\text{-S-C}_6\text{H}_5$  radical. If the yield of the decarboxylation from the sulfur-centered radical zwitterion is taken to be 100%, then the extinction coefficient of  $\cdot\text{CH}_2\text{-S-C}_6\text{H}_5$  would be  $\epsilon(330 \text{ nm}) = 5500 \text{ M}^{-1} \text{ cm}^{-1}$ , taking  $G(\text{C}_6\text{H}_5\text{-S}^{\bullet+}\text{-CH}_2\text{-CO}_2^-) = 2.15$ ; see above. Our previously<sup>15</sup> reported extinction coefficient,  $\epsilon(330 \text{ nm}) = 4200 \text{ M}^{-1} \text{ cm}^{-1}$ , was based on  $G(\text{C}_6\text{H}_5\text{-S}^{\bullet+}\text{-CH}_2\text{-CO}_2^-) = 2.65$ .

With the new reference spectrum of  $\cdot\text{CH}_2\text{-S-C}_6\text{H}_5$  and the reference spectra for  $\text{CB}^{\bullet-}$  and  $\text{CBH}^{\bullet}$ , it was possible to reproduce the time-resolved transient spectra following the quenching of  $^3\text{CB}^*$  by  $\text{C}_6\text{H}_5\text{-S-CH}_2\text{-CO}_2^-$  at pH 7.5. It was not possible to resolve reliably any sulfur-centered radical zwitterion component on any time scale. However, the  $\cdot\text{CH}_2\text{-S-C}_6\text{H}_5$  shows a significantly large, extrapolated quantum yield of about 0.93; see Table 1. The extrapolation is only approximate as can be seen from the concentration profile in Figure 2. The  $\cdot\text{CH}_2\text{-S-C}_6\text{H}_5$  radical's concentration profile shows that this radical has formed quite rapidly within 1  $\mu\text{s}$  of the laser pulse, which is consistent with any initially formed  $\text{C}_6\text{H}_5\text{-S}^{\bullet+}\text{-CH}_2\text{-CO}_2^-$  decaying rapidly, as in the pulse radiolysis experiments:



Furthermore, the large quantum yield of  $\cdot\text{CH}_2\text{-S-C}_6\text{H}_5$  is consistent with the S-centered radical zwitterion being formed in the quenching event with a large quantum yield that matches the large initial quantum yield of  $\text{CB}^{\bullet-}$  (0.97, see Table 1) and the large quantum yield of  $\text{CO}_2$  (0.92) in previously reported steady-state photolysis experiments.<sup>10</sup> Argued another way, the

large quantum yield of  $\text{CB}^{\bullet-}$  would indicate that a comparable amount of  $\text{C}_6\text{H}_5\text{-S}^{\bullet+}\text{-CH}_2\text{-CO}_2^-$  would be formed, and the large steady-state yield of  $\text{CO}_2$  would be consistent with this radical decarboxylating, i.e., eq 8. The radical anion  $\text{CB}^{\bullet-}$  persists well for hundreds of microseconds as can be seen in kinetic traces at 650 nm.

**Quenching of  $^3\text{CB}^*$  by  $\text{C}_6\text{H}_5\text{-CH}_2\text{-S-CH}_2\text{-CO}_2^-$ .** Triplet CB is also quenched quite rapidly by  $\text{C}_6\text{H}_5\text{-CH}_2\text{-S-CH}_2\text{-CO}_2^-$  at pH 7.2. The triplet quenching rate constant is  $k_q = 1.5 \times 10^9 \text{ M}^{-1} \text{ s}^{-1}$ ; see Table 1. Again this suggests electron transfer is the likely quenching mechanism.

In preparation for resolving any transient spectra following rapid quenching of the triplet state, pulse radiolysis experiments were performed to collect reference spectra. These experiments and the reactions involved were analogous to the ones described above (see eqs 3–6). The purpose was to determine the spectra of the S-centered radical zwitterion,  $\text{C}_6\text{H}_5\text{-CH}_2\text{-S}^{\bullet+}\text{-CH}_2\text{-CO}_2^-$ , and the C-centered radical,  $^{\bullet}\text{CH}_2\text{-S-CH}_2\text{-C}_6\text{H}_5$ , formed following decarboxylation of the S-centered radical zwitterion. The resulting spectrum, following pulse radiolysis, shows transient absorption only below 360 nm. There is a distinct band/shoulder at 295 nm that is typical of  $\alpha$ -(alkylthio)alkyl radicals. This contribution to the transient spectra is likely due to the  $^{\bullet}\text{CH}_2\text{-S-CH}_2\text{-C}_6\text{H}_5$  radical. The absorption continues upward at shorter wavelengths even to 260 nm. In addition there is a very sharp absorption feature at 315 nm that is likely due to the benzyl radical  $^{\bullet}\text{CH}_2\text{-C}_6\text{H}_5$ ; see below. These observations indicate that the sulfur-centered radical zwitterions,  $\text{C}_6\text{H}_5\text{-CH}_2\text{-S}^{\bullet+}\text{-CH}_2\text{-CO}_2^-$ , are not stable on a time scale less than our time resolution. They either fragment or decay via decarboxylation [as observed for monomeric sulfur radical cations derived from 2-(methylthio)ethanoic and 2,2'-thiodiethanoic acids].<sup>16</sup>

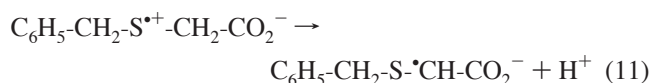
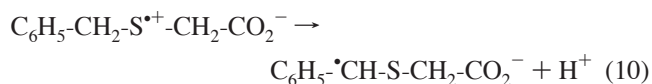
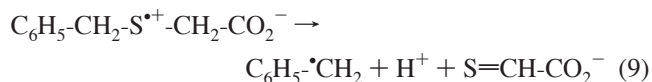
On the other hand, the radicals  $\text{C}_6\text{H}_5\text{-}^{\bullet}\text{CH-S-CH}_2\text{-CO}_2^-$  and  $\text{C}_6\text{H}_5\text{-CH}_2\text{-S-}^{\bullet}\text{CH-CO}_2^-$ , potentially formed from the deprotonation of the sulfur-centered radical zwitterions, do not appear to be present in the pulse radiolysis experiments because of the lack of transient absorptions above 360 nm. DFT calculations (in the gas phase) indicate that  $\text{C}_6\text{H}_5\text{-}^{\bullet}\text{CH-S-CH}_2\text{-CO}_2^-$  has transitions at 540 nm ( $f = 0.03$ ) and 335 nm ( $f = 0.17$ ) and that  $\text{C}_6\text{H}_5\text{-CH}_2\text{-S-}^{\bullet}\text{CH-CO}_2^-$  has weak transitions at 486 nm ( $f = 0.01$ ) and 435 nm ( $f = 0.01$ ). The lack of any such transitions suggests that deprotonations of  $\text{C}_6\text{H}_5\text{-CH}_2\text{-S}^{\bullet+}\text{-CH}_2\text{-CO}_2^-$  leading to these radicals are not significant.

The spectral resolutions of the transient spectra following triplet quenching by **2** showed only  $\text{CB}^{\bullet-}$  and  $\text{CBH}^{\bullet}$ . It is not too surprising that  $\text{C}_6\text{H}_5\text{-CH}_2\text{-S}^{\bullet+}\text{-CH}_2\text{-CO}_2^-$  was not seen in laser photolysis studies because its lifetime was too short-lived to be observed even in the pulse radiolysis experiments. However, the relatively large yield (0.57, see Table 1) of  $\text{CO}_2$  in the steady-state, photosensitization experiments<sup>10</sup> suggests that there should be  $^{\bullet}\text{CH}_2\text{-S-CH}_2\text{-C}_6\text{H}_5$  radicals present in significant amounts. The issue is complicated in the laser flash experiments because CB starts absorbing below 360 nm, which complicates spectral resolutions with ground-state bleaching of CB. The  $^{\bullet}\text{CH}_2\text{-S-CH}_2\text{-C}_6\text{H}_5$  radical's maximum (about 300 nm) is shifted significantly to the blue from that of  $^{\bullet}\text{CH}_2\text{-S-C}_6\text{H}_5$  ( $\lambda_{\text{max}} = 330 \text{ nm}$ )<sup>15</sup> so as to put it out of the observed spectral range needed for reliable resolution of components. For instance, the  $^{\bullet}\text{CH}_2\text{-S-CH}_2\text{-C}_6\text{H}_5$  radical absorbs only below 400 nm and then only weakly ( $<200 \text{ M}^{-1} \text{ cm}^{-1}$ ) above 360 nm. With such a weak absorption and such a small number of wavelengths available, it was not possible to get reliable spectral resolutions including  $^{\bullet}\text{CH}_2\text{-S-CH}_2\text{-C}_6\text{H}_5$  in the spectral mix. To get reliable quantum yields for  $\text{CB}^{\bullet-}$  and  $\text{CBH}^{\bullet}$ , the spectral resolutions were

performed between 400 and 800 nm. This is why only  $\text{CB}^{\bullet-}$  and  $\text{CBH}^{\bullet}$  show up in the final spectral mix; see Figure 3 for the resulting concentration profiles.

The quenching events following the  $^3\text{CB}^*$ -sensitized oxidation of  $\text{C}_6\text{H}_5\text{-CH}_2\text{-S-CH}_2\text{-CO}_2^-$  are thus not too different from those with  $\text{C}_6\text{H}_5\text{-S-CH}_2\text{-CO}_2^-$  as the quencher. In both cases, it can be inferred that S-centered radical zwitterions are formed because of the complementary high yields of radical anions  $\text{CB}^{\bullet-}$  (see Table 1). It is plausible that the S-centered radical zwitterions are not seen in the laser flash experiments because of their rapid decay, which is analogous to the observations and interpretation of the corresponding pulse radiolysis experiments. DFT calculations do show that decarboxylation of  $\text{C}_6\text{H}_5\text{-CH}_2\text{-S}^{\bullet+}\text{-CH}_2\text{-CO}_2^-$  is exothermic by 12 kcal/mol in the gas phase. Even though the dipole moment of the zwitterions radical is large, the decarboxylation reaction is still exothermic in solution.

However, the decay modes of the S-centered radical zwitterions may vary in the two cases as indicated by the difference in  $\text{CO}_2$  yields in Table 1. For  $\text{C}_6\text{H}_5\text{-S-CH}_2\text{-CO}_2^-$ , the  $\text{CO}_2$  quantum yield (0.92) is very close to the quantum yield (0.97) of  $\text{CB}^{\bullet-}$ , indicating that its S-centered radical zwitterion decays almost exclusively by decarboxylation. On the other hand, when  $\text{C}_6\text{H}_5\text{-CH}_2\text{-S-CH}_2\text{-CO}_2^-$  is the quencher, the  $\text{CO}_2$  quantum yield (0.57) is significantly less than the quantum yield (0.83) of  $\text{CB}^{\bullet-}$ . [Note that in the case of the aliphatic analogue,  $\text{CH}_3\text{-S-CH}_2\text{-CO}_2^-$ , the quantum yield values for  $\text{CO}_2$  and  $\text{CB}^{\bullet-}$  are equal ( $\Phi_{\text{CO}_2} = 0.86$  and  $\Phi_{\text{CB}^{\bullet-}} = 0.87$ ), indicating that decarboxylation is the only reaction of  $\text{CH}_3\text{-S}^{\bullet+}\text{-CH}_2\text{-CO}_2^-$ .<sup>16</sup>] The difference between  $\Phi_{\text{CO}_2}$  and  $\Phi_{\text{CB}^{\bullet-}}$  in the  $\text{C}_6\text{H}_5\text{-CH}_2\text{-S}^{\bullet+}\text{-CH}_2\text{-CO}_2^-$  radical could be due to its increased tendency to decay by fragmentation<sup>40</sup> and deprotonation:

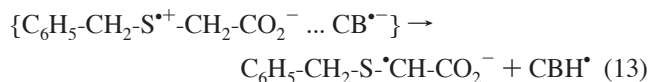
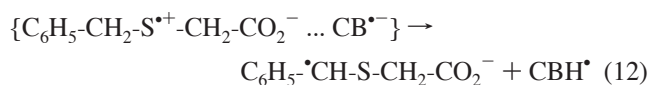


A plausible explanation for the difference in decarboxylation yields in **1** and **2** is the fragmentation in eq 9. This reaction is also driven by the solvation of the proton on the right-hand side of the reaction. The stabilization of the benzyl radical is also an enabling factor. This explanation has the added advantage that the benzyl radical appears as a component in the observed transient spectra from the pulse radiolysis experiments.

No DFT-computed transitions of the deprotonated radicals in eqs 10 and 11 were definitively identified in the transient spectra following pulse radiolysis of **2** (see above). However, because the discrepancy in photoinduced decarboxylation in **1** vs **2** is so prominent, it is important to take a closer look at deprotonations as alternate reaction pathways to decarboxylation. In general, the magnitude of the activation energy for deprotonation is dominated by the solvation of the reaction products, i.e., protons and anion radicals in eqs 10 and 11. Since solvations in eqs 10 and 11 should be similar, the relative stabilization of the product radicals would be the determining factor in this case. A rough idea of the relative importance of the deprotonation of  $\text{C}_6\text{H}_5\text{-CH}_2\text{-S}^{\bullet+}\text{-CH}_2\text{-CO}_2^-$  vs  $\text{C}_6\text{H}_5\text{-S}^{\bullet+}\text{-CH}_2\text{-CO}_2^-$  can be

illustrated by looking at the relative stabilization energies ( $\Delta H$ ) of  $\text{C}_6\text{H}_5\text{-}\dot{\text{C}}\text{H-S-CH}_2\text{-CO}_2^-$  vs  $\text{C}_6\text{H}_5\text{-CH}_2\text{-S-}\dot{\text{C}}\text{H-CO}_2^-$ , the latter of which might be considered to be representative of  $\text{C}_6\text{H}_5\text{-S-}\dot{\text{C}}\text{H-CO}_2^-$  from compound **1**. DFT computations indicate that  $\text{C}_6\text{H}_5\text{-}\dot{\text{C}}\text{H-S-CH}_2\text{-CO}_2^-$  is more stable by 7 kcal/mol with respect to  $\text{C}_6\text{H}_5\text{-CH}_2\text{-S-}\dot{\text{C}}\text{H-CO}_2^-$  in the gas phase and 3 kcal/mol in solution. Although the relative stabilization energies do slightly favor the  $\text{C}_6\text{H}_5\text{-}\dot{\text{C}}\text{H-S-CH}_2\text{-CO}_2^-$  radical compared to the  $\text{C}_6\text{H}_5\text{-CH}_2\text{-S-}\dot{\text{C}}\text{H-CO}_2^-$  radical (and by analogy  $\text{C}_6\text{H}_5\text{-S-}\dot{\text{C}}\text{H-CO}_2^-$ ), it is not sufficient to make a convincing rationalization that would account for the observed decrease in decarboxylation of **2** compared to **1**, particularly in the absence of definitive evidence for the existence of the deprotonated radicals in the observed transient spectra, see above.

On the other hand, the deprotonation sites, discussed above, could be operative in the collision complexes,  $\{\text{C}_6\text{H}_5\text{-CH}_2\text{-S}^{+\bullet}\text{-CH}_2\text{-CO}_2^- \dots \text{CB}^{\bullet-}\}$ , whereby the S-centered radical zwitterions could transfer a proton to  $\text{CB}^{\bullet-}$ , forming  $\text{CBH}^\bullet$  and a C-centered radical:



The intrinsic deprotonation of the S-centered radical zwitterion (eqs 10 and 11) may not be important, that is, there is no clear evidence of their presence in the transient spectra from pulse radiolysis. However, the deprotonation of  $\text{C}_6\text{H}_5\text{-CH}_2\text{-S}^{+\bullet}\text{-CH}_2\text{-CO}_2^-$  in the collision complex (eqs 12 and 13) serves as an additional source of C-centered radicals (Scheme 1) with a quantum yield equal to that of the ketyl radical ( $\text{CBH}^\bullet$ ) (Table 1).

**Quenching of  $^3\text{CB}^*$  by  $\text{CH}_3\text{-S-C}_6\text{H}_4\text{-CH}_2\text{-CO}_2^-$ .** The rate constant for quenching  $^3\text{CB}^*$  by  $\text{CH}_3\text{-S-C}_6\text{H}_4\text{-CH}_2\text{-CO}_2^-$  in neutral aqueous solution is  $1.9 \times 10^9 \text{ M}^{-1} \text{ s}^{-1}$ . Anticipating that electron-transfer transients would contribute to the transient spectra following the quenching event, pulse radiolysis experiments were performed to acquire reference spectra for the sulfur-centered radical zwitterion,  $\text{CH}_3\text{-S}^{+\bullet}\text{-C}_6\text{H}_4\text{-CH}_2\text{-CO}_2^-$ , and the C-centered radical,  $\dot{\text{C}}\text{H}_2\text{-C}_6\text{H}_4\text{-S-CH}_3$ , formed, as argued below, from the decarboxylation of the sulfur-centered radical zwitterion.

In pulse radiolysis experiments of **3**, the characteristic absorptions for monomeric radical cations were seen at 320 and 560 nm. This particular S-centered radical zwitterion,  $\text{CH}_3\text{-S}^{+\bullet}\text{-C}_6\text{H}_4\text{-CH}_2\text{-CO}_2^-$ , lived for longer than 10  $\mu\text{s}$  (see inset to Figure 5). However, due to the necessarily low concentration (0.2 mM) of its precursor,  $\text{CH}_3\text{-S-C}_6\text{H}_4\text{-CH}_2\text{-CO}_2^-$ , the experimental growth was only  $9.3 \times 10^5 \text{ s}^{-1}$  compared to its decay of  $1.7 \times 10^5 \text{ s}^{-1}$ , on the basis of a growth/decay fit

$$\Delta A = \Delta A_\infty \{\exp(-k_{\text{decay}} t) - \exp(-k_{\text{growth}} t)\} \quad (14)$$

to the kinetic trace at 560 nm; see inset to Figure 5. A 560-nm trace on a 20- $\mu\text{s}$  time scale was also fit with similar rate constants; this longer time scale gave a better sampling of points in the decay and a poorer sampling of points in the growth section of its kinetic trace. From the fitting parameter,  $\Delta A_\infty = 0.0106$  at 560 nm, and the dosimetry ( $[\text{SO}_4^{\bullet-}]_0 = 1.53 \mu\text{M}$ ), the extinction coefficient  $\epsilon(560 \text{ nm})$  was calculated:

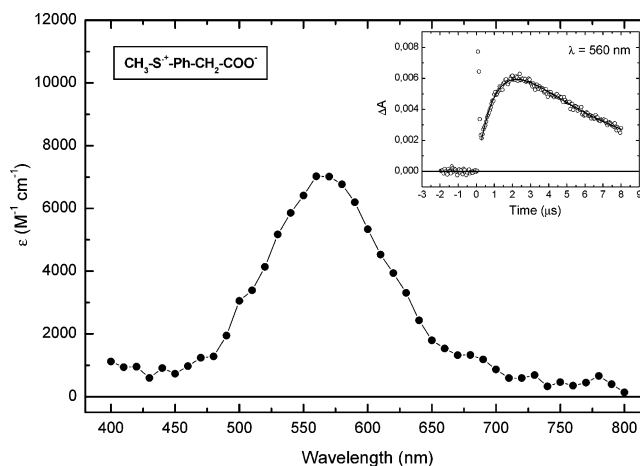


**Figure 5.** Reference spectrum of  $\text{CH}_3\text{-S}^{+\bullet}\text{-C}_6\text{H}_4\text{-CH}_2\text{-CO}_2^-$ :  $\epsilon_{560} = 7000 \text{ M}^{-1} \text{ cm}^{-1}$ , recorded 2–3  $\mu\text{s}$  following pulse radiolysis of an  $\text{N}_2$ -saturated aqueous solution, pH 5.5, for 0.2 mM  $\text{CH}_3\text{-S-C}_6\text{H}_4\text{-CH}_2\text{-CO}_2^-$  (**3**), 2 mM  $\text{Na}_2\text{S}_2\text{O}_8$ , and 0.1 M  $t\text{-BuOH}$ . Inset shows experimental trace for growth and decay of the  $\text{CH}_3\text{-S}^{+\bullet}\text{-C}_6\text{H}_4\text{-CH}_2\text{-CO}_2^-$  taken at 560 nm.

$$\epsilon_{560}(\text{S}^{+\bullet}) = \frac{\Delta A_\infty}{l[\text{SO}_4^{\bullet-}]_0} \frac{k_{\text{growth}} - k_{\text{decay}}}{k_{\text{growth}}} \frac{2.65}{2.15} \quad (15)$$

The result is  $7000 \text{ M}^{-1} \text{ cm}^{-1}$  for  $\text{CH}_3\text{-S}^{+\bullet}\text{-C}_6\text{H}_4\text{-CH}_2\text{-CO}_2^-$ , under the following assumptions: (i) that only the  $\text{S}^{+\bullet}$  radical absorbs at 560 nm; (ii) that the scavenging reaction 5 is 100% efficient, with  $G(\text{SO}_4^{\bullet-}) = 2.65$  radicals per 100 eV of absorbed energy; and (iii) that scavenging reaction 4 is only 81% efficient with  $G(\text{S}^{+\bullet}) = 2.15$  radicals per 100 eV of absorbed energy.<sup>15</sup> Equations 14 and 15 come from the solution of the linear differential equation for the kinetics:

$$\frac{d[\text{S}^{+\bullet}]}{dt} = k_{\text{growth}}[\text{SO}_4^{\bullet-}] - k_{\text{decay}}[\text{S}^{+\bullet}] \quad (16)$$

with  $\text{SO}_4^{\bullet-}$  decaying exponentially,  $[\text{SO}_4^{\bullet-}]_t = [\text{SO}_4^{\bullet-}]_0 \exp\{-k_{\text{growth}} t\}$ , and with initial conditions  $[\text{SO}_4^{\bullet-}]_{t=0} = [\text{SO}_4^{\bullet-}]_0$  and  $[\text{S}^{+\bullet}]_{t=0} = 0$ .

In the pulse radiolysis experiments, the kinetic trace at 320 nm is very long-lived and must include at least one extra species in addition to the contribution from the  $\text{S}^{+\bullet}$  radical. An obvious candidate is the radical from the decarboxylation of the  $\text{S}^{+\bullet}$  radical, as mentioned above. Such a radical would be a substituted benzyl radical,  $\dot{\text{C}}\text{H}_2\text{-C}_6\text{H}_4\text{-S-CH}_3$ . The benzyl radical itself has strong, sharp absorptions<sup>41</sup> in this very region, which supports the tentative spectral assignment. DFT calculations also show a very strong transition at 315 nm ( $f = 0.26$ ) for  $\dot{\text{C}}\text{H}_2\text{-C}_6\text{H}_4\text{-S-CH}_3$  with a much weaker transition at 427 nm ( $f = 0.05$ ). The transient spectrum remaining at around 110  $\mu\text{s}$  after the electron pulse contains a weak absorption remaining in the spectral region  $\lambda > 400 \text{ nm}$ , which we also assign to the  $\dot{\text{C}}\text{H}_2\text{-C}_6\text{H}_4\text{-S-CH}_3$  radicals, as argued below.

The 320-nm kinetic trace (in pulse radiolysis) showed an additional time constant on the order of 50  $\mu\text{s}$ , indicating the presence of a third radical, possibly the radical obtained from deprotonation of  $\text{CH}_3\text{-S}^{+\bullet}\text{-C}_6\text{H}_4\text{-CH}_2\text{-CO}_2^-$ . One such radical,  $\dot{\text{C}}\text{H}_2\text{-S-C}_6\text{H}_4\text{-CH}_2\text{-CO}_2^-$ , would be expected to have an absorption spectrum similar to that for the  $\dot{\text{C}}\text{H}_2\text{-S-C}_6\text{H}_5$  radicals, i.e., little or no absorption for  $\lambda > 400 \text{ nm}$ . DFT computations show (gas-phase) transitions at 347 nm ( $f = 0.03$ ), 363 nm ( $f = 0.04$ ), 368 nm ( $f = 0.05$ ), and 402 nm ( $f = 0.01$ ). A similar calculation on  $\text{CH}_3\text{-S-C}_6\text{H}_4\text{-}\dot{\text{C}}\text{H-CO}_2^-$  does show a relatively strong transi-



tion with an oscillator strength of 0.05 at 415 nm and a much weaker one at 338 nm. (This radical might not be expected to arise directly from deprotonation of  $\text{CH}_3\text{-S}^+\text{-C}_6\text{H}_4\text{-CH}_2\text{-CO}_2^-$ , but it could be important in the triplet-quenching experiments; see below.)

From these considerations, the substituted benzyl radical from the decarboxylation of  $\text{CH}_3\text{-S}^+\text{-C}_6\text{H}_4\text{-CH}_2\text{-CO}_2^-$  is the most likely radical remaining after 100  $\mu\text{s}$  following the radiolytic pulse. By  $t = 100 \mu\text{s}$ , the  $\text{CH}_3\text{-S}^+\text{-C}_6\text{H}_4\text{-CH}_2\text{-CO}_2^-$  radical has disappeared (see inset to Figure 5), and at this delay time, two lifetimes have lapsed for the third radical, probably  $\text{CH}_2\text{-S-C}_6\text{H}_4\text{-CH}_2\text{-CO}_2^-$ , absorbing at 320 nm.

Thus the spectral shape of the substituted benzyl radical is taken to be the transient absorption at 110  $\mu\text{s}$ . An estimate of its extinction coefficient was made by use of the quantum yield of  $\text{CO}_2$  formation (see Table 1) and the preliminary estimates for the quantum yield of  $\text{S}^{++}$  from the triplet-quenching data. The assumption is that  $\text{S}^{++}$  can decay into parallel channels, deprotonation and decarboxylation. The radiolytic yield  $G(\text{substituted benzyl})$  can then be taken to be equal to  $2.15 \times$  quantum yield of  $\text{CO}_2/\text{quantum yield of } \text{S}^{++}$ ; namely, the results from the triplet-sensitized photolysis experiments are used as a means of estimating the radiation yield of the substituted benzyl radical. From this estimate of the  $G(\text{substituted benzyl})$ , the spectrum of this radical was quantified.

For simplicity the spectral resolutions (from laser flash photolysis) were carried out between 400 and 800 nm, which avoids most of the complications with the C-centered radicals. Only the tail of the substituted benzyl radical needs to be considered above 400 nm. It also avoids the need of disentangling all three radicals derived from **3** in the spectral region below 400 nm. The  $\text{CH}_2\text{-S-C}_6\text{H}_4\text{-CH}_2\text{-CO}_2^-$  does not absorb above 400 nm, and the other two radicals can be separated on the basis of their distinctive time-dependent behavior and their slight spectral overlap, as long as only the spectral region above 400 nm is considered. The transient spectrum at 2–3  $\mu\text{s}$  after the electron pulse between 400 and 800 nm was taken as the true shape of  $\text{S}^{++}$  for compound **3**; see Figure 5. This time interval is optimal not only because the absorption from  $\text{S}^{++}$  is maximal but also because  $\text{SO}_4^{\cdot-}$  has decayed and because the C-centered radicals have yet to accumulate significantly.

With the use of the newly obtained reference spectrum of  $\text{CH}_3\text{-S}^+\text{-C}_6\text{H}_4\text{-CH}_2\text{-CO}_2^-$  in Figure 5, the transient spectra, following  $^3\text{CB}^*$  quenching events, were resolved into components, i.e.,  $\text{CB}^{\cdot-}$ ,  $\text{CBH}^{\cdot}$ , and  $\text{S}^{++}$ , with 400–800 nm taken as a region for spectral resolution. Our initial resolutions gave rough agreement between the data and the fitted spectra that were reconstructed from the component reference spectra, each of which was weighted with the regression parameters. The fits appeared to be skewed relative to the observed transient spectra by the lack of any components that could contribute significant absorption in the near-infrared spectral region.

Since  $\text{CH}_3\text{-S}^+\text{-C}_6\text{H}_4\text{-CH}_2\text{-CO}_2^-$  radicals are present and some of the laser flux is being absorbed by the quencher (see above), it seemed prudent to determine whether the near-infrared contributions could be due to hydrated electrons from direct photoionization of the solute. A 12 mM neutral, aqueous solution of  $\text{CH}_3\text{-S-C}_6\text{H}_4\text{-CH}_2\text{-CO}_2^-$  was photolyzed with 337-nm pulsed laser excitation. The resulting transient spectra are shown in Figure 6. The contribution from the  $\text{S}^{++}$  radical is clearly present, particularly at 550 nm in the spectrum taken in the time window from 1 to 1.5  $\mu\text{s}$ , i.e., note the similarity to the reference spectrum in Figure 5. In this same time window it can be seen, in Figure 6, that the absorption in the near-infrared is still

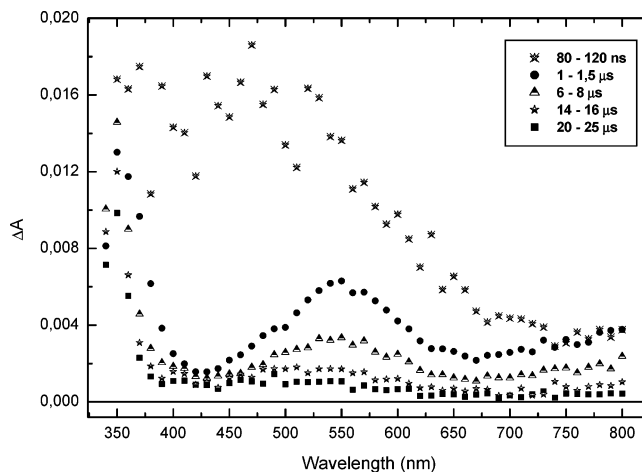


**Figure 6.** Transient spectrum following 337-nm laser flash photolysis of  $\text{CH}_3\text{-S-C}_6\text{H}_4\text{-CH}_2\text{-CO}_2^-$  (**3**) (12 mM), in Ar-saturated aqueous solution, pH = 6.91, recorded at five different delays times; relative actinometry,  $[\text{T}] = 24.8 \mu\text{M}$ .

prominent. Attempts to resolve these transient spectra were not very successful, even after the short-lived, near-UV component decays significantly. However, the bulk of the remaining spectrum appears to be accounted for by the  $\text{S}^{++}$  radical and a species absorbing in the near-infrared. The short-lived transient is likely due to triplet–triplet absorption. It is quenched by oxygen with a rate constant of approximately  $5 \times 10^9 \text{ M}^{-1} \text{ s}^{-1}$ , computed from eq 7 with the  $k_{\text{obs}}$  measured in a pure oxygen-saturated solution and  $\tau_0$  measured in an argon-saturated solution. The near-infrared species should have also been quenched by oxygen if this absorption was due to the hydrated electron, but no such scavenging was observed. In addition, no enhanced decay rate was observed in the 700–800 nm range when the solutions were saturated with  $\text{N}_2\text{O}$ , an excellent scavenger of hydrated electrons. Both of these observations with oxygen and  $\text{N}_2\text{O}$  would argue against hydrated electrons being responsible for the infrared transient.

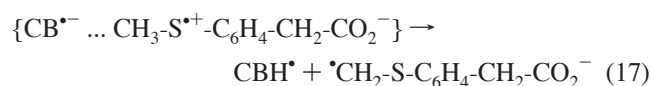
Although we have not been able to identify the nature of the infrared transient, we were able to obtain a very rough spectral shape for it. This was possible because the lifetime of its decay (5.4  $\mu\text{s}$ ) is much shorter than all the other radicals (except for  $\text{S}^{++}$ , which has a fitted decay time of  $1/1.7 \times 10^5 \text{ s}^{-1}$  from the inset of Figure 5). Therefore subtracting the observed transient spectrum at a delay time  $t =$  four lifetimes ( $4 \times 5.4 \mu\text{s}$ ) from the transient spectrum at  $t = 5.4 \mu\text{s}$  leaves a difference spectrum containing only  $\text{S}^{++}$  and the infrared transient. By use of this difference spectrum and the spectrum of  $\text{S}^{++}$  in Figure 5, the spectrum of the infrared transient was extracted iteratively. This was done by starting with the assumption that the contribution of  $\text{S}^{++}$  was the same as that of  $\text{S}^{++}$  from a preliminary spectral resolution at 5.4  $\mu\text{s}$ , where the spectrum of the hydrated electron was used as a first approximation to the infrared transient's spectrum. The resulting spectral shape of the infrared transient is given as the dashed line in Figure 1; the scale is necessarily arbitrary since its concentration and extinction coefficient are unknown. With this near-infrared component, the concentration profiles associated with  $\text{CH}_3\text{-S-C}_6\text{H}_4\text{-CH}_2\text{-CO}_2^-$  quenching  $^3\text{CB}^*$  are presented in Figure 4 with one of the spectral resolutions given in Figure 1. Only the shape of the unknown infrared transient is required to obtain quantitative results for the other transients, each of which has known extinction coefficients. In Table 1, all of the quantum yields of transient species in these experiments with the quencher  $\text{CH}_3\text{-S-C}_6\text{H}_4\text{-}$



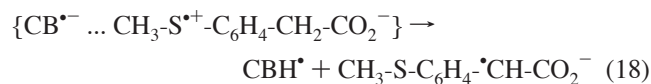
$\text{CH}_2\text{-CO}_2^-$  are computed on the basis of the light absorbed by CB only; see eq 2.

Analysis of the results, in Figure 4 and Table 1 for quencher **3**, leads to the following conclusions: (i)  $\text{CB}^{\bullet-}$  is one of the main primary photochemical products ( $\Phi_{\text{CB}^{\bullet-}} = 0.71$ ); (ii) the quantum yield of  $\text{CH}_3\text{-S}^{\bullet+}\text{-C}_6\text{H}_4\text{-CH}_2\text{-CO}_2^-$  formation was determined to be  $\Phi_{\text{S}^{\bullet+}} = 0.90$ , in agreement with the value of  $\text{CB}^{\bullet-}$  formation; and (iii) decay of the  $\text{S}^{\bullet+}$  radical occurs on the microsecond time scale, similar to its decay in pulse radiolysis (Figure 5). The lack of exact agreement in the yields of  $\text{CB}^{\bullet-}$  and  $\text{S}^{\bullet+}$  could be due to the  $\text{S}^{\bullet+}$  formed in the direct photolysis of **3** as described above.

Although  $\text{CBH}^{\bullet}$  could arise from H-abstraction via  $^3\text{CB}^*$ , H-abstraction via aromatic ketones is usually much slower<sup>42</sup> than the triplet quenching rate constants that we have observed in this work. Thus it seems more probable that the H-abstraction products that we have observed come from electron transfer followed by proton transfer in the collision complex:

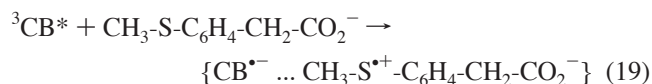


or

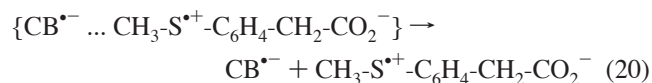


The  ${}^{\bullet}\text{CH}_2\text{-S-C}_6\text{H}_4\text{-CH}_2\text{-CO}_2^-$  radical is an  $\alpha$ -thioalkyl radical such as  ${}^{\bullet}\text{CH}_2\text{-S-C}_6\text{H}_5$ . In the pulse radiolysis experiments involving  $\text{CH}_3\text{-S-C}_6\text{H}_4\text{-CH}_2\text{-CO}_2^-$ , the yield of these  $\alpha$ -thioalkyl radicals or  $\text{CH}_3\text{-S-C}_6\text{H}_4\text{-}^{\bullet}\text{CH-CO}_2^-$  radicals might be not as prominent as it would be from a true sulfur radical cation because of the lack of a driving force for deprotonation of the overall neutral species,  $\text{CH}_3\text{-S}^{\bullet+}\text{-C}_6\text{H}_4\text{-CH}_2\text{-CO}_2^-$ . However, the photochemical experiments, with the presence of the doubly charged radical anion,  $\text{CB}^{\bullet-}$ , as its collision partner,  $\text{CH}_3\text{-S}^{\bullet+}\text{-C}_6\text{H}_4\text{-CH}_2\text{-CO}_2^-$  might be induced to behave much more like a true sulfur radical cation that deprotonates readily from its  $\alpha$ -carbons.

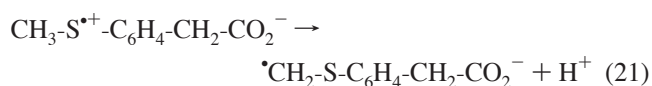
The quantum yields in Table 1 can be discussed in the context of quenching of  $^3\text{CB}^*$  via electron transfer within the collision complex (see Scheme 1)



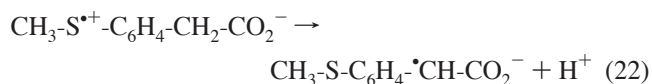
followed by escape of the radical anion and S-centered radical zwitterion from the collision complex



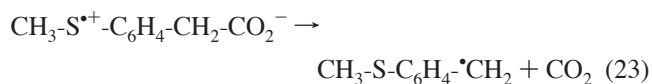
which is in competition with protonation within the collision complex, followed by escape of radicals (eqs 17 and 18). According to this mechanism, the quantum yield  $\Phi_{\text{S}^{\bullet+}} = 0.90$  (from Table 1) for the formation of  $\text{S}^{\bullet+}$  radicals should be the same as the yield for the formation of  $\text{CB}^{\bullet-}$  ( $\Phi_{\text{CB}^{\bullet-}} = 0.71$ ). The quantum yield of  $\text{CO}_2$  from steady-state photosensitization experiments<sup>10</sup> was recomputed for inner-filter effects. The corrected quantum yield of 0.40 is less than the value of the quantum yield for the formation of  $\text{S}^{\bullet+}$  radicals ( $\Phi_{\text{S}^{\bullet+}} = 0.90$ ). This indicates that in addition to decarboxylation, the sulfur-centered radical zwitterions may undergo deprotonation



or



with a combined efficiency ( $0.90 - 0.40 = 0.50$ ) similar to that for decarboxylation (0.40):



Although the analysis was iterative, these final quantum yields for the parallel processes, deprotonation vs decarboxylation, support the assumptions made in determining the quantitative spectrum of the  $\text{CH}_3\text{-S-C}_6\text{H}_4\text{-}^{\bullet}\text{CH}_2$  radical (see above). The deprotonated radicals  ${}^{\bullet}\text{CH}_2\text{-S-C}_6\text{H}_4\text{-CH}_2\text{-CO}_2^-/\text{CH}_3\text{-S-C}_6\text{H}_4\text{-}^{\bullet}\text{CH-CO}_2^-$  can be formed in reactions 21/22, unimolecularly, and also within the collision complex, reactions 17/18, respectively. The deprotonation reactions within the collision complexes should correspond to the yield of  $\text{CBH}^{\bullet}$  extrapolated to time zero. From Table 1 this value is 0.017. Thus if deprotonations were the only alternative decay channels to  $\text{S}^{\bullet+}$ , the overall quantum yield of  ${}^{\bullet}\text{CH}_2\text{-S-C}_6\text{H}_4\text{-CH}_2\text{-CO}_2^-$  and  $\text{CH}_3\text{-S-C}_6\text{H}_4\text{-}^{\bullet}\text{CH-CO}_2^-$  should be equal to the sum of the yield (0.50) from unimolecular  $\text{S}^{\bullet+}$  deprotonation (reactions 21/22) and the yield (0.017) from intercomplex deprotonation (reactions 17/18), i.e.,  $\Phi \approx 0.52$ . The quantum yield ( $\approx 0.5$ , Table 1) of the substituted benzyl radical computed from the maximum of its growth/decay concentration profile in Figure 5 is consistent with this number.

Comparative stabilization (from DFT calculations) of the deprotonated radicals  ${}^{\bullet}\text{CH}_2\text{-S-C}_6\text{H}_4\text{-CH}_2\text{-CO}_2^-$  and  $\text{CH}_3\text{-S-C}_6\text{H}_4\text{-}^{\bullet}\text{CH-CO}_2^-$  is 12 kcal/mol in favor of the latter. This should make  $\text{CH}_3\text{-S-C}_6\text{H}_4\text{-}^{\bullet}\text{CH-CO}_2^-$  the likely product in the intercomplex deprotonation (reaction 18) where there is an external base, i.e.,  $\text{CB}^{\bullet-}$ .

On the other hand, in the unimolecular deprotonations (reactions 21/22), it is not clear that the Evans/Polanyi rule<sup>43</sup> (activation energies follow stabilization energies) would apply. It is well-known that deprotonations are relatively facile at carbons adjacent to cationic sulfur radical centers (reaction 21), which is in contrast to a distant deprotonation on the other side of the aromatic ring (reaction 22). Thus we expect that reaction 21 (formation of  ${}^{\bullet}\text{CH}_2\text{-S-C}_6\text{H}_4\text{-CH}_2\text{-CO}_2^-$ ) would be favored over reaction 22 in unimolecular deprotonations of  $\text{CH}_3\text{-S}^{\bullet+}\text{-C}_6\text{H}_4\text{-CH}_2\text{-CO}_2^-$ .

Escape of the radicals in eq 20 involves the escape of a doubly charged radical anion ( $\text{CB}^{\bullet-}$ ) from a neutral radical with a large dipole,  $\text{CH}_3\text{-S}^{\bullet+}\text{-C}_6\text{H}_4\text{-CH}_2\text{-CO}_2^-$ . It might be expected that escape of such a pair would be easier than in the usual case of  $^3\text{CB}^*$  quenching when true radical cations are involved. From Table 1 it is seen that all the quenchers in this study have much larger quantum yields of  $\text{CB}^{\bullet-}$  than of  $\text{CBH}^{\bullet}$ . This supports the expectation that the ion-dipole collision complexes should be relatively easy to separate, e.g., eq 20.

**Quenching of  $^3\text{CB}^*$  by  $\text{CH}_3\text{-S-C}_6\text{H}_4\text{-CO}_2^-$ .** The quenching of  $^3\text{CB}^*$  by  $\text{CH}_3\text{-S-C}_6\text{H}_4\text{-CO}_2^-$  is again quite rapid,  $1.9 \times 10^9 \text{ M}^{-1} \text{ s}^{-1}$ . Pulse radiolysis was used to obtain reference spectra of the sulfur radical zwitterion and its decay products. The absorption spectrum in the range 400–800 nm is dominated

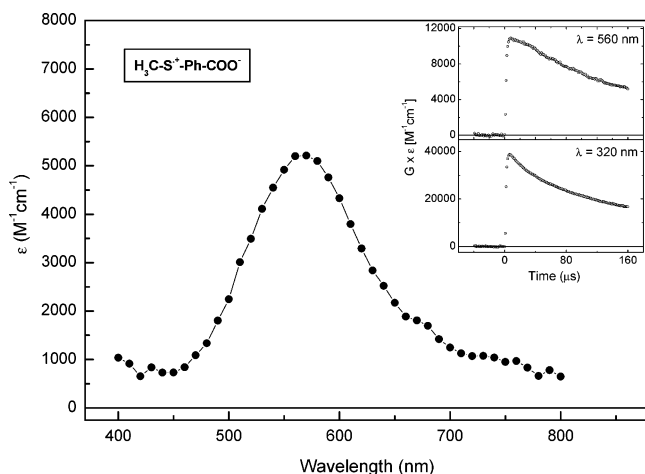


**Figure 7.** Reference spectrum of  $\text{CH}_3\text{-S}^{\bullet+}\text{-C}_6\text{H}_4\text{-CO}_2^-$ :  $\epsilon_{560} = 5200 \text{ M}^{-1} \text{ cm}^{-1}$ , recorded 120–140  $\mu\text{s}$  following pulse radiolysis of an  $\text{N}_2$ -saturated aqueous solution, pH 5.5, for 0.2 mM  $\text{CH}_3\text{-S-C}_6\text{H}_4\text{-COO}^-$  (**4**), 2 mM  $\text{Na}_2\text{S}_2\text{O}_8$ , and 0.1 M *t*-BuOH. Insets show experimental decay traces at 560 nm (top inset) and 320 nm (bottom inset).

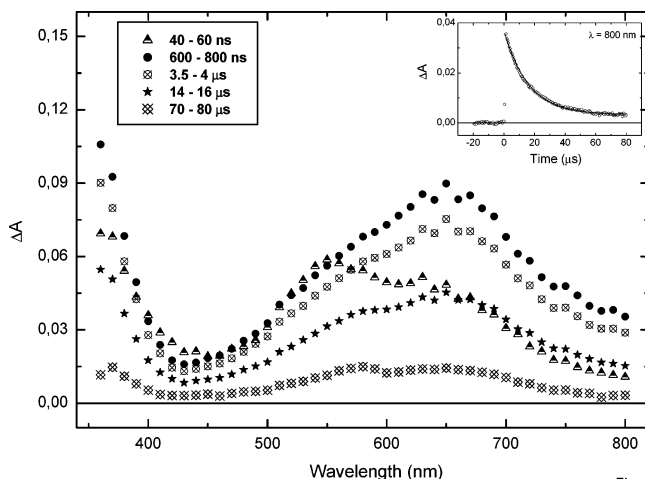


**Figure 8.** Transient spectra following triplet quenching of CB by  $\text{CH}_3\text{-S-C}_6\text{H}_4\text{-CO}_2^-$  (**4**) (5 mM) + CB (4 mM) in Ar-saturated aqueous solution, pH = 6.91; actinometry,  $[\text{T}] = 16.3 \mu\text{M}$ . Inset: Kinetic trace at 800 nm.

by the absorption of the S-centered radical zwitterion,  $\text{CH}_3\text{-S}^{\bullet+}\text{-C}_6\text{H}_4\text{-CO}_2^-$ , with  $\lambda_{\text{max}} = 560 \text{ nm}$  and  $\epsilon_{560} = 5200 \text{ M}^{-1} \text{ cm}^{-1}$  (Figure 7). The kinetic traces at 560 and 320 nm in the pulse radiolysis are distinctly different (see insets to Figure 7). The decay at 560 nm is slow while the decay at 320 nm has a rapidly decaying component in addition to the long-lived decay. The extra radical may be the deprotonated radical  $^{\bullet}\text{CH}_2\text{-S-C}_6\text{H}_4\text{-CO}_2^-$ , having a computed transition energy of 295 nm from DFT (gas phase) with a very large oscillator strength ( $f = 0.4$ ).

In the laser-initiated triplet-sensitization experiments, the transient spectra following the quenching events are shown in Figure 8. No transient absorptions ascribable to decarboxylation products were seen either in the pulse radiolysis of pH 5.5 aqueous solutions of  $\text{CH}_3\text{-S-C}_6\text{H}_4\text{-CO}_2^-$  (with 0.1 M *tert*-butyl alcohol and 2 mM  $\text{Na}_2\text{S}_2\text{O}_8$ ,  $\text{N}_2$ -saturated) or in the laser flash photolysis triplet-quenching experiments. This is consistent with the steady-state photosensitization experiments<sup>10</sup> that detected no  $\text{CO}_2$ ; see Table 1. The failure of the  $\text{CH}_3\text{-S}^{\bullet+}\text{-C}_6\text{H}_4\text{-CO}_2^-$  radical to decarboxylate is likely related to the high energy of activation needed to form the substituted phenyl radical that would be the product from decarboxylation of  $\text{CH}_3\text{-S}^{\bullet+}\text{-C}_6\text{H}_4\text{-CO}_2^-$ . DFT computations indicate that, in the gas phase,  $\text{CH}_3\text{-S}^{\bullet+}\text{-C}_6\text{H}_4\text{-CO}_2^-$  is 12 kcal/mol more stable than the *p*-meth-

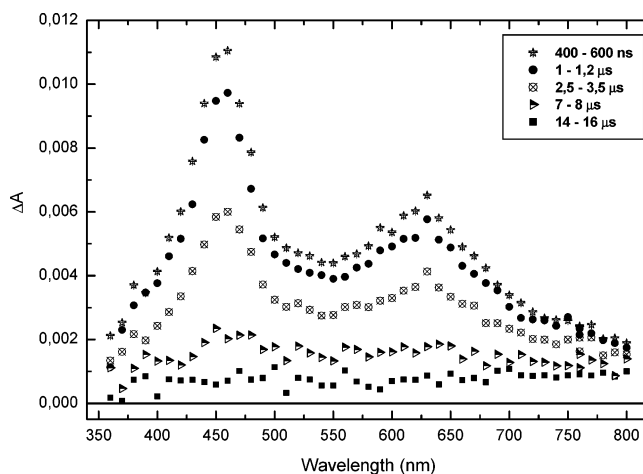


**Figure 9.** Transient spectra following 337-nm laser flash photolysis of  $\text{CH}_3\text{-S-C}_6\text{H}_5\text{-CO}_2^-$  (**4**) (10 mM), in Ar-saturated aqueous solution, pH = 7.32;  $[\text{T}] = 12.8 \mu\text{M}$ , recorded after five different delay times.

ylthiophenyl radical and  $\text{CO}_2$ . The solution-phase dipole moment of  $\text{CH}_3\text{-S}^{\bullet+}\text{-C}_6\text{H}_4\text{-CO}_2^-$  is 6 D (from DFT), further stabilizing this zwitterion radical to decarboxylation.

There is a significant transient absorption at wavelengths longer than 750 nm, which is the limit of significant absorption from  $\text{CB}^{\bullet-}$ . Since  $\text{CH}_3\text{-S-C}_6\text{H}_4\text{-CO}_2^-$  absorbs approximately 9% of the laser photons at 337 nm, the possibility of photoionization needs to be addressed. Pulsed, 337-nm direct excitation of a 10 mM solution of  $\text{CH}_3\text{-S-C}_6\text{H}_4\text{-CO}_2^-$  at pH 7.32 was performed. The resulting transient spectra are displayed in Figure 9. The absorptions decay uniformly over the entire displayed spectral range, indicating that there is only a single species present. There is some absorption in the vicinity of the hydrated electron's absorption, but this absorption decays in the same pattern as the main two bands. The entire transient absorption is quenched by pure oxygen. The oxygen quenching rate constant of  $2.3 \times 10^9 \text{ M}^{-1} \text{ s}^{-1}$  was determined, by use of eq 7, with the lifetime ( $1/k_{\text{obs}}$ ) measured at this single oxygen concentration (solution purged with pure oxygen) and the lifetime ( $\tau_0$ ) measured in an argon-saturated solution. This is consistent with the transient being the triplet-triplet absorption of the substrate.

Further evidence indicating that the long-wavelength absorption was not due to hydrated electrons was given from transient spectra following quenching events when exactly the same composition system (10 mM in **4**, pH 7.3) was saturated with  $\text{N}_2\text{O}$ . The transient spectra were indistinguishable from the argon-saturated solutions.

The triplet-sensitized experiments were also repeated with  $\text{N}_2\text{O}$ -saturated solutions. There were no detectable differences between these transient spectra and those in the argon-saturated solutions. The kinetic traces of the argon-saturated solutions were fit with various functional forms. At most of the wavelengths the decays were second-order, indicating a radical nature of the species. However, the unknown transient absorbing beyond 750 nm decayed by a first-order process. The lifetime of the 800-nm kinetic trace of this transient was 15  $\mu\text{s}$  (see inset to Figure 8). Work is underway in these laboratories to investigate the nature of the infrared transients in compounds **3** and **4**.

## Conclusions

By observing complementary electron-transfer products in pulse radiolysis, steady-state photolysis, and laser flash photolysis, it was inferred that the sulfur-centered radical zwitterions

from **1** and **2** decayed rapidly (faster than our time resolution of a few nanoseconds). The sulfur-centered radical zwitterions from **1** decayed into the products,  $\bullet\text{CH}_2\text{-S-C}_6\text{H}_5$  and  $\text{CO}_2$ , that were observed in pulse radiolysis and steady-state photolysis, respectively. A majority (57%) of the sulfur-centered radical zwitterions ( $\text{S}^+$ ) from **2** also decayed via decarboxylation, and in addition, they decayed through a fragmentation channel. DFT calculations of optical transitions of possible C-centered radicals derived from the  $\text{S}^{++}$  radicals of **2** helped eliminate deprotonation as a major decay channel for the  $\text{S}^+$  radicals of **2**. The  $\text{CH}_3\text{-S}^+-\text{C}_6\text{H}_4\text{-CH}_2\text{-CO}_2^-$  radicals from **3** could be observed directly for microseconds and decayed with roughly equal probability through decarboxylation and deprotonation. The  $\text{CH}_3\text{-S}^+-\text{C}_6\text{H}_4\text{-CO}_2^-$  radicals from **4** were also observed directly but failed to decarboxylate because of the high energy of activation needed to form the substituted phenyl radical. The zwitterionic nature of the sulfur-centered radicals in this work was indicated by their large dipole moments as computed by DFT.

**Acknowledgment.** This work was supported by the Committee for Scientific Research, Poland (Grant 3TO 9A 03719 and by the Office of Basic Energy Sciences of the U.S. Department of Energy. Work supported in part by the European Community's Human Potential Program under Contract HPRN-CT-2002-00184 (SULFRAD). This is Document NDRL 4476 from the Notre Dame Radiation Laboratory.

## References and Notes

- Wrzyszczyński, A.; Scigalski, F.; Paczkowski, J. *Nukleonika* **2000**, 45, 73–81.
- Chatgililoglu, C.; Bertrand, M. P.; Ferreri, C. Sulfur-centered radicals in organic synthesis. In *S-centered Radicals*; Alfassi, Z. B., Ed.; John Wiley & Sons Ltd.: Chichester, U.K., 1999; pp 311–354.
- Bauld, N. L.; Aplin, J. T.; Yueh, W.; Loinaz, A. *J. Am. Chem. Soc.* **1997**, 119, 11381–11389.
- Wardman, P. Thiyl Radicals in Biology: Their Role as a 'Molecular Switch' central to Cellular Oxidative Stress. In *S-centered Radicals*; Alfassi, Z. B., Ed.; John Wiley & Sons Ltd.: Chichester, U.K., 1999; pp 289–309.
- Berlett, B.; Stadtman, E. R. *J. Biol. Chem.* **1997**, 272, 20313–20316.
- Schöneich, C. *Exp. Gerontol.* **1999**, 34, 19–34.
- Tobien, T.; Cooper, W. J.; Nickelsen, M. G.; Pernas, E.; O'Shea, K. E.; Asmus, K.-D. *Environ. Sci. Technol.* **2000**, 34, 1286–1291.
- Urbanski, S. P.; Wine, P. H. Chemistry of Gas Phase Organic Sulfur-centered Radicals. In *S-centered Radicals*; Alfassi, Z. B., Ed.; John Wiley & Sons Ltd.: Chichester, U.K., 1999; pp 97–140.
- Speight, V. L.; Balchou, E. R.; Nixon, E. M. *Florida Wat. Resour. J.* **1997**, 25–26.
- Wrzyszczyński, A.; Filipiak, P.; Hug, G. L.; Marciniak, B.; Paczkowski, J. *Macromolecules* **2000**, 33, 1577–1582.
- Bonifacic, M.; Möckel, H.; Bahnmann, D.; Asmus, K.-D. *J. Chem. Soc., Perkin Trans. 2* **1975**, 675–685.
- Mönig, J.; Goslich, R.; Asmus, K.-D. *Ber. Bunsen-Ges. Phys. Chem.* **1986**, 90, 115–121.
- Asmus, K.-D. *Acc. Chem. Res.* **1979**, 12, 436–442.
- Ioele, M.; Steenken, S.; Baciocchi, E. *J. Phys. Chem. A* **1997**, 101, 2979–2987.
- Korzeniowska-Sobczuk, A.; Hug, G. L.; Carmichael, I.; Bobrowski, K. *J. Phys. Chem. A* **2002**, 106, 9251–9260.
- Marciniak, B.; Bobrowski, K.; Hug, G. L.; Rozwadowski, J. *J. Phys. Chem.* **1994**, 98, 4854–4860.
- Hug, G. L.; Bobrowski, K.; Kozubek, H.; Marciniak, B. *Photochem. Photobiol.* **1998**, 68, 785–796.
- Thomas, M. D.; Hug, G. L. *Comput. Chem. (Oxford)* **1998**, 22, 491–498.
- Hug, G. L.; Wang, Y.; Schöneich, C.; Jiang, P.-Y.; Fessenden, R. W. *Radiat. Phys. Chem.* **1999**, 54, 559–566.
- Mirkowski, J.; Wisniowski, P.; Bobrowski, K. INCT Annual Report 2000, Institute of Nuclear Chemistry and Technology, 2000.
- Janata, E.; Schuler, R. H. *J. Phys. Chem.* **1982**, 86, 2078–2084.
- Frisch, M. J.; Trucks, G. W.; Schlegel, H. B.; Scuseria, G. E.; Robb, M. A.; Cheeseman, J. R.; Zakrzewski, V. G.; Montgomery, J. A., Jr.; Stratmann, R. E.; Burant, J. C.; Dapprich, S.; Millam, J. M.; Daniels, A. D.; Kudin, K. N.; Strain, M. C.; Farkas, O.; Tomasi, J.; Barone, V.; Cossi, M.; Cammi, R.; Mennucci, B.; Pomelli, C.; Adamo, C.; Clifford, S.; Ochterski, J.; Petersson, G. A.; Ayala, P. Y.; Cui, Q.; Morokuma, K.; Malick, D. K.; Rabuck, A. D.; Raghavachari, K.; Foresman, J. B.; Cioslowski, J.; Ortiz, J. V.; Baboul, A. G.; Stefanov, B. B.; Liu, G.; Liashenko, A.; Piskorz, P.; Komaromi, I.; Gomperts, R.; Martin, R. L.; Fox, D. J.; Keith, T.; Al-Laham, M. A.; Peng, C. Y.; Nanayakkara, A.; Gonzalez, C.; Challacombe, M.; Gill, P. M. W.; Johnson, B.; Chen, W.; Wong, M. W.; Andres, J. L.; Head-Gordon, M.; Replogle, E. S.; Pople, J. A. *Gaussian 98*; Gaussian, Inc.: Pittsburgh, PA, 1998.
- Becke, D. A. *J. Chem. Phys.* **1993**, 98, 5648–5652.
- Slater, J. C. *The Self-Consistent Field for Molecules and Solids*; McGraw-Hill: New York, 1974.
- Becke, A. D. *ACS Symp. Ser.* **1989**, 394, 165–179.
- Vosko, S. H.; Wilk, L.; Nusair, M. *Can. J. Phys.* **1980**, 58, 1200–1211.
- Lee, C.; Yang, W.; Parr, R. G. *Phys. Rev. B* **1988**, 37, 785–789.
- Hariharan, P. C.; Pople, J. A. *Chem. Phys. Lett.* **1972**, 16, 217–219.
- Casida, M. E.; Jamorski, C.; Casida, K. C.; Salahub, D. R. *J. Chem. Phys.* **1998**, 108, 4439–4449.
- Reed, A. E.; Weinstock, R. B.; Weinhold, F. *J. Chem. Phys.* **1985**, 83, 735–746.
- Barone, V.; Cossi, M. *J. Phys. Chem. A* **1998**, 102, 1995–2001.
- Klamt, A.; Schuurmann, G. *J. Chem. Soc., Perkin Trans. 2* **1993**, 799–805.
- Marciniak, B.; Bobrowski, K.; Hug, G. L. *J. Phys. Chem.* **1993**, 97, 11937–11943.
- Carmichael, I.; Hug, G. L. *J. Phys. Chem. Ref. Data* **1986**, 15, 1–250.
- Parker, C. A. *Photoluminescence of Solutions*; Elsevier: Amsterdam, 1968.
- Baciocchi, E.; Bietti, M.; Putignani, L.; Steenken, S. *J. Am. Chem. Soc.* **1996**, 118, 5952–5960.
- Buxton, G. V.; Greenstock, C. L.; Helman, W. P.; Ross, A. B. *J. Phys. Chem. Ref. Data* **1988**, 17, 513–886.
- Inbar, S.; Linschitz, H.; Cohen, S. G. *J. Am. Chem. Soc.* **1981**, 103, 1048–1054.
- Hurley, J. K.; Linschitz, H.; Treinin, A. *J. Phys. Chem.* **1988**, 92, 5151–5159.
- Baciocchi, E.; Bietti, M.; Lanzalunga, O. *Acc. Chem. Res.* **2000**, 33, 243–251.
- Bobrowski, K. *J. Phys. Chem.* **1981**, 85, 382–388.
- Scaiano, J. C. *J. Photochem.* **1973/74**, 2, 81–118.
- Evans, M. G.; Polanyi, M. *Trans. Faraday Soc.* **1935**, 31, 875.